Sub-100-Hz DFB Laser Injection-Locked to PM Fiber Ring Cavity

Ivan S. Panyaev [ID], Pavel A. Itrin [ID], Dmitry A. Korobko [ID], and Andrei A. Fotiadi [ID]

Abstract—**Low-noise lasers are invaluable tools in applications ranging from precision spectroscopy and displacement measurements to the development of advanced optical atomic clocks. Although all these applications benefit from reduced frequency noise, some also demand a low-cost and robust design. In this article, we introduce a novel and practical concept of a simple, single-frequency laser that utilizes a ring fiber cavity for self-injection locking of a standard semiconductor distributed feedback (DFB) laser. Contrary to previously reported solutions, our laser configuration is fully spliced from polarization-maintaining (PM) single-mode optical fiber components. This results in an adjustment- and maintenance-free narrow-band laser operation with significantly enhanced stability against environmental noise. Importantly, continuous-wave (CW) single-frequency laser operation is achieved through self-injection locking, while the low-bandwidth active optoelectronic feedback serves exclusively to maintain this regime. Operating with output powers of $\sim$8 mW, the proposed fiber configuration narrows the natural Lorentzian linewidth of the emitted light to $\sim$ 75 Hz and ensures phase and intensity noise levels of less than – 120 dBc/Hz ($>$ 10 kHz) and – 140 dBc/Hz ($>$ 30 kHz), respectively. Furthermore, the thermally stabilized laser exhibits a frequency drift of less than $\sim$ 0.5 MHz/min with a maximal frequency walk-off of $<$ 8 MHz. We believe that translating this laser design to integrated photonics in the near future could dramatically lower costs and reduce the footprint in various applications, including ultra-high-capacity fiber and data center networks, atomic clocks, and microwave photonics.**

Index Terms—**Fiber ring cavity, laser linewidth, narrow-band fiber lasers, self-injection locking.**

I. INTRODUCTION

RECENTLY, ultra-narrow-band light sources have emerged as pivotal components in advancing optical communication [1], [2], [3], optical precision measurement [4], [5], [6],

[7], [8], and signal synthesis [9], owing to their extended coherency length and minimal phase noise. The laser linewidth, a critical parameter for characterizing the coherence of a laser light source, has garnered significant research attention [10], [11]. A variety of narrow-band laser configurations have been proposed, utilizing either active optoelectronic feedback [12], [13] or passive optical feedback [14]. In the context of optoelectronic feedback, the narrowing of the laser linewidth primarily hinges on laser frequency stabilization technology. This technology relies on the electrical circuit's capability to offset the frequency disparity between the laser and the reference frequency. However, this type of laser frequency stabilization is technically challenging and often cost-prohibitive for more widespread laser applications.

The optical feedback method utilizes the self-injection locking mechanism, offering a significant enhancement in the spectral performance of standard DFB lasers [15], [16], [17]. To achieve this effect, a portion of the optical radiation emitted by the laser passes through an external cavity, which acts as a narrow-band filter, before being reintroduced into the laser cavity. This process lowers the laser threshold at the ring resonant frequency, leading to a marked reduction in laser linewidth [18], [19], [20], [21], [22]. In this context, a longer cavity length is beneficial for improving the laser's linewidth, making ring cavities based on optical fibers [23] an appropriate choice. A laser with a kHz linewidth can be constructed simply by integrating a standard distributed feedback (DFB) laser diode with several passive telecommunication components [24], [25], [26]. While the linewidth of a typical free-running DFB semiconductor laser varies from a few MHz to tens of MHz [27], self-injection locking via an external fiber ring cavity can narrow the laser's linewidth to just a few kHz, or even less. This efficient approach facilitates the design of cost-effective narrow-band laser sources using standard laser diodes, positioning them as an attractive alternative to traditional laser systems that utilize active feedback [28], [29], [30], [31], [32], [33].

This technique, however, presents a significant drawback. Owing to the small intermode distance and the extended feedback loop, it's highly susceptible to fluctuations in both configuration parameters and environmental conditions [34]. When the laser locks onto the ring cavity resonance, it starts operating at the ring resonant frequency, adjusting to its gradual shifts. Yet, influenced by environmental vibrations and thermal dynamics noise, the laser frequency deviates from the external cavity resonance. This deviation can ultimately lead to mode hopping, where the locked laser frequency oscillates between the external

Ivan S. Panyaev, Pavel A. Itrin, and Dmitry A. Korobko are with the Ulyanovsk State University, 432017 Ulyanovsk, Russia (e-mail: panyaev.ivan@rambler.ru; itrin@mail.ru; korobkotam@rambler.ru).

Andrei A. Fotiadi is with the Optoelectronics and Measurement Techniques Unit, University of Oulu, 90570 Oulu, Finland, and also with the University of Mons, 7000 Mons, Belgium (e-mail: andrei.fotiadi@oulu.fi).

ring cavity modes, temporarily undermining the laser's stable operation [35]. To address this issue, various strategies have been pursued to stabilize the laser operation within the self-injection locking regime. Relying solely on optical feedback, stable laser operation typically persists for just a few seconds. However, by meticulously controlling the laser diode current and temperature, in conjunction with regulating the temperature of the entire fiber setup, one can prolong stable laser operation to several tens of minutes or even longer [36]. Nonetheless, these stabilization techniques are intricate and tend to be more expensive.

Recently, we demonstrated a laser stabilization concept that achieves significant DFB laser linewidth narrowing through self-injection locking to an external fiber ring cavity. In these laser configurations, the locked laser frequency is stabilized to the cavity resonance via the active control of phase delay in the optical feedback fiber that returns light to the DFB laser cavity [37]. To this end, the optical feedback fiber is equipped with a phase-shifter [38]. This device continuously adjusts the laser phase to compensate for any mismatches between the DFB laser's operating frequency and the ring cavity resonance caused by environmental noise. In the active optoelectronic feedback circuit, the optical power detected from one of the laser outputs can act as the error signal used by a cost-effective USB-DAQ card controlling the phase shifter. Importantly, in contrast to previously reported lasers with optoelectronic circuit feedback, our approach hinges on the linewidth narrowing effect solely induced by the self-injection-locking mechanism. The active feedback is utilized just to maintain the laser's operation within the self-injection-locking regime. As a result, our method is considerably less resource-intensive in terms of feedback circuit bandwidth, complexity, and memory allocation compared to traditional optoelectronic systems associated with fiber lasers [39], [40].

Over the past several years, this innovative approach has led to significant advancements, achieving sub-kHz laser linewidths and paving the way for advanced applications such as distributed fiber sensors [41]. We have also introduced a series of Brillouin lasers using the same mechanism. In these dual-wavelength configurations, an external fiber ring cavity serves two primary functions: it acts as a narrow-band filter, facilitating self-injection locking of the DFB laser, and as a medium for Brillouin scattering [42], [43], [44], [45], [46], [47], [48], generating Stokes-shifted optical waves. Notably, our recent Brillouin laser configuration [49] employs a fiber ring cavity constructed from a single fiber coupler, departing from the traditional use of two couplers. This approach gives the system both simplicity and an enhanced cavity Q-factor. Through the application of thermal control to the entire laser configuration, we have achieved stable laser performance, ensuring continuous, mode-hopping-free operation. When pumped with a standard DFB laser diode, this configuration emits a sub-100-Hz laser linewidth at the Brillouin frequency. Although it does so with sub-milliwatt output power, the primary DFB laser emits power of ∼5 mW with a linewidth close to 400 Hz. This characteristic makes the laser especially suitable for dual-wavelength applications, such as distributed fiber Brillouin sensing [50], [51], [52]. However, for applications that rely on a single-wavelength laser and need a sub-100-Hz
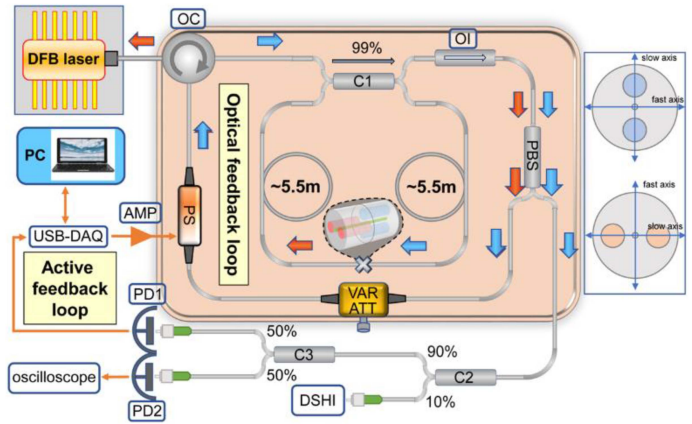

Fig. 1. Schematic illustration of the experimental configuration; OC – optical circulator, C1 – optical PM fiber coupler (both axes working), OI – optical isolator, PBS – polarizing beam splitter, VAR ATT – variable attenuator (0 – 60 dB), PS – phase shifter, C2 and C3 – non-PM single-mode fiber couplers, PD1 and PD2 – photodetectors, USB-DAQ – microcontroller, AMP – electric amplifier. DSHI – delayed self-heterodyne interferometer. The highlighted area bounded by the dashed line indicates the thermal stabilization box. On the right is shown the orientation of the fiber birefringence axes on either side of the splice.

laser linewidth, this configuration may not be the most practical choice. Furthermore, this laser setup, constructed from standard optical fiber, requires meticulous adjustments to maintain its desired operational mode. Even with these adjustments, it remains sensitive to prolonged environmental changes and often requires periodic recalibrations.

In this work, we address these limitations and demonstrate a robust sub-100-Hz single-wavelength continuous-wave (CW) laser source. This source employs a standard DFB laser diode self-injection-locked to an external ring fiber cavity. Unlike previously reported solutions, our new laser configuration comprises exclusively polarization-maintaining (PM) fiber components. To minimize the operational linewidth, we have managed to build the PM laser configuration using a fiber ring cavity spliced from a single fiber coupler. This simplified all-PM-fiber laser design renders the laser more resistant to external perturbations and environmental noise. It also eliminates the need for polarization controllers within the cavity, making the laser configuration robust and adjustment-free. Based on this, we experimentally investigate and verify the proposed narrow-band PM fiber laser solution, demonstrating control and tuning of the laser linewidth down to 75 Hz. We successfully achieved an ultra-narrow linewidth laser with phase and intensity noise reduced to – 120 dBc/Hz (> 10 kHz) and – 140 dBc/Hz (> 30kHz), respectively. Additionally, we elucidate the physical mechanisms underlying laser stabilization, linewidth narrowing, and phase noise reduction. This paves the way for precise control over laser spectral and polarization characteristics under conditions of controllable coherence.

II. LASER CONFIGURATION

The experimental laser setup built from standard telecom components is shown in Fig. 1. A standard DFB laser diode
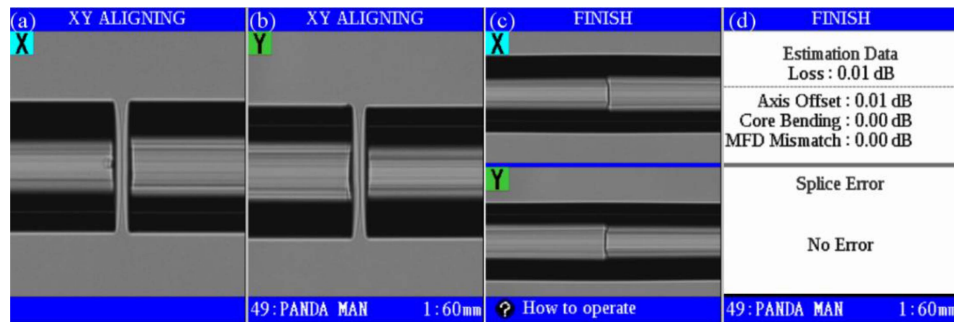
Fig. 2. Images of the PM fibers spliced with rotation of their birefringence axes by 90° relative to each other inside the ring fiber cavity (as marked by a cross in Fig. 1) before [(a) and (b)] and after splicing [(c) and (d)].

(Mitsubishi Electric Corp., FU-68PDF-V510M67B) supplied by a −30 dB built-in optical isolator generates radiation with a maximal power of ∼ 15 mW at ∼ 1552 nm ($T_d = 25\,°C$) in linear polarization. The laser radiation passes through the optical circulator (OC), 99/1 fiber coupler (C1), optical isolator (OI), polarization beam splitter (PBS), variable attenuator (VAR ATT), delay fiber with the inserted phase shifter (PS) and again circulator (OC) returns back into the DFB laser cavity thus providing passive optical feedback to the DFB laser operation. The fiber ring cavity serving as a narrow-band optical pass filter is a part of the optical feedback loop. It is spliced from the 99/1 PM coupler (C1) with ∼11.33 m of a standard PM fiber (Nufern PM1550-XP). The polarization beam splitter redirects a part of the laser power to the laser output and a fast photodetector that is a part of the electronic feedback circuit. The circulator and optical isolators prevent the DFB laser from undesirable back reflections from the fiber faces. The most sensitive part of the laser configuration (red marked area in Fig. 2) is placed into a foam box, protecting the system from environmental noise. The laser operation is monitored by a fast photodetector (PD, Thorlabs DET08CFC, 5 GHz, 800 - 1700 nm).

Although, the laser configuration shown in Fig. 1 looks like a single-wavelength version of the one reported in [49], several crucial solutions have been implemented to improve qualitatively the laser performance. The new configuration is entirely spliced from PM fiber components. The robust PM laser design excludes polarization controllers, making the laser adjustment-free and more suitable for practical applications. To enable the operation of optical feedback loop in this case, the fixed distribution of the light polarization state over the laser configuration is imposed directly by proper splicing of the PM fiber components. In particular, the ring fiber cavity is built by splicing the ends of the fiber PM coupler with the rotation of their birefringence axes by 90° (as marked by a cross in Fig. 1). Fig. 2 shows the images of the splicing process with the Fujikura FSM-100P splicing machine. Two left images show the alignment of the fiber ends with rotation of the birefringence axes by 90° before splicing, whereas two right images show the spliced fibers. So, the fiber ring cavity is formed by two PM fiber segments of the same length (∼ 5.5 m) optically connected by the coupler C1 on one side and spliced together with the birefringence axes rotated by 90° relative to each other on the

other side. When the DFB laser light circulates in the fiber ring cavity, its polarization state undergoes a rotation by 90° after each round trip, i.e., the radiation polarized along the slow PM fiber axis after a round occurs polarized along the fast fiber axis and versa.

For the CW laser light circulating inside the ring cavity, the optical power is averaged over polarizations and equally shared between the fast and slow fiber axes, making a minor difference between them. However, when the light is extracted from the ring through the coupler, only one of the polarization components (that coincides with the DFB laser polarization state) interferes with the DFB laser radiation at the coupler output. The polarization beam splitter (PBS) specified with the polarization extinction ratio > 23 dB separates two polarization components and redirects them into two individual PM fiber outputs, each polarized along the slow fiber axis. The light in the first fiber with the polarization state coinciding with the DFB laser is split between the laser output and a fast photodetector that provides an error signal employed by the optoelectronic feedback circuit. The second fiber containing the light with the polarization initially orthogonal to the DFB laser is the fiber delay line equipped with the phase shifter (PS). At the end, it is spliced with the optical circulator (OC) to inject the light into the DFB laser cavity in the polarization of the DFB laser thus preventing the polarization switching inside the laser cavity. The portion of the power injected into the DFB laser cavity is controlled by the variable attenuator (with attenuation up to 60 dB). Typically, the variable attenuator is set to a transparency level of 30% or higher.

The optoelectronic feedback circuit helps the laser to maintain the laser operation in self-injection-locking regime. The thermo-optical fiber phase shifter (Phoenix Photonics VPS150-15-PM-2-1) inserted into the fiber feedback loop is driven by a low-cost USB Multifunction DAQ (based on the Arduino board) connected with a PC. With the voltage applied to the phase shifter, the DAQ continuously tunes the phase delay in the optical feedback loop trying to minimize the error signal provided by the photodetector. It is worth noting that the use of the fiber phase-shifter based on thermo-optical effect is helpful due to its low cost and extended dynamical range ∼150π rad. In contrast to the mechanical piezo-activator used in our previous experiments [38], [49], it does not introduce acoustic vibrations that have
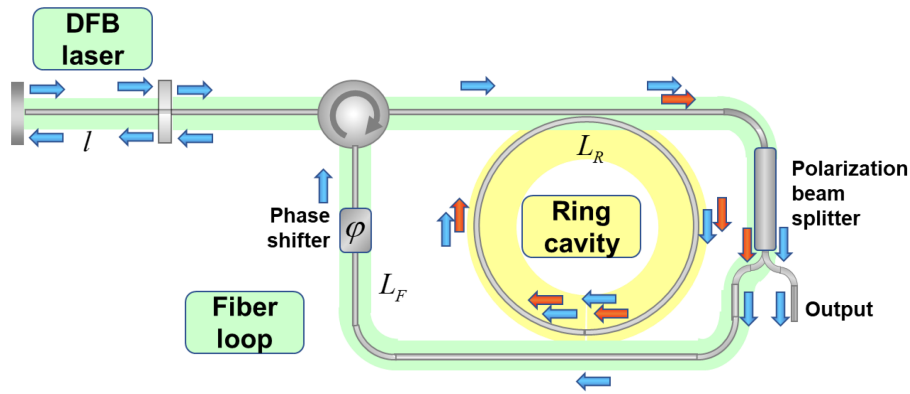
Fig. 3. Illustration to the self-injection locking laser operation. Green background shows the coupled cavity comprising the DFB laser and feedback loop possessing the resonance at ν_{LD+FD}; yellow background marks the ring cavity with the resonance at ν_R. Arrows show the polarization states along the fast (red) and slow (blue) axes.

been found to impair the laser performance characteristics. An additional thermal control (also based on the Arduino board) is applied to the laser box stabilizing it at $\sim 30 \pm 0.01$ ^{0}C to keep the phase-shifter within its dynamic range.

III. LASER OPERATION AND STABILIZATION

The principle of the self-injection locking mechanism with filtered optical feedback is explained in [15], [16], [17]. The isolation afforded by the built-in DFB laser isolator emerges as a crucial parameter in the laser models [23]. To enable a stable injection locking, the isolation should typically range between -25 and -35 dB, which aligns with the standard isolation of single-stage optical fiber isolators. A simplified view of the laser operation is illustrated in Fig. 3. The laser configuration is thought as the DFB laser optically coupled with two external fiber cavities marked by green and yellow backgrounds, respectively. The light emitted by a DFB laser passes the fiber ring cavity and the optical feedback loop. It is injected back into the DFB laser cavity, forcing the DFB laser to emit at $\nu_L = \nu_R$, where ν_R is one of the ring cavity resonant frequencies. For stable operation, the laser frequency ν_L should be simultaneously resonant in two cavities: the ring cavity (ν_R) and the coupled cavity comprising the DFB laser cavity and feedback loop (ν_{LD+FB}), i.e., $\nu_L = \nu_R = \nu_{LD+FB}$. The phase shifter tunes the position of the frequency ν_{LD+FB} relative ν_R according to the applied voltage. The laser vicinity to the resonance is monitored through the laser pump power detected by the photodetector, producing the error signal. As the laser system approaches the resonance, the laser light circulating inside the cavity exhibits a strong enhancement in its power, resulting in an increase in the feedback signal and a decrease in the power detected by the photodetector. The laser operation becomes unstable when the environment noise affecting the laser configuration fibers violates the equality $\nu_R = \nu_{LD+FB}$. The task of the active feedback circuit is to maintain the equality, minimizing the error signal detected by the photodetector.

In general, there are two cases when mode-hopping in the laser occurs. The first is a mechanical vibration, such as a flick on the

laser box, that causes short-time perturbations of the laser power. To protect the laser configuration from mechanical vibrations, it is enclosed in a foam box. The second is an extended temperature drift. While the active feedback circuit operates to counteract temperature drift, the voltage applied to the phase shifter could exhaust its dynamic range ($\sim 150\pi$ rad). In this case, for further operation, the phase delay induced by the phase shifter should be reset by an integer number of 2π. Such a jump destabilizes the laser in the same way as the flick on the box. To avoid destabilization, the phase shifter's working point should always be maintained within its dynamic range. It is achieved with the additional thermal stabilization of the laser box. It is worth noting that in this ensemble, the voltage applied to the phase shifter could be simultaneously used as an error signal for getting advanced thermal control.

IV. EXPERIMENTAL RESULTS

A. Active Stabilization Technique

With the laser configuration shown in Fig. 1 the output power is monitored by the photodetector. The signal from the photodetector is also used as an error signal for the operation of the optoelectronic feedback circuit. Fig. 4 highlights the work of active optoelectronic feedback circuit by demonstrating oscilloscope traces recorded simultaneously with the laser output power (error signal) and active feedback voltage applied to the phase shifter. Fig. 4(a) compares the dynamics of laser power before and after the active optoelectronic circuit is switched-on (at the moment of T = 0 s). For the laser operating without active feedback (T< 0 s) no driving signal is applied to the phase shifter (Uc = const) and the DFB laser frequency is not locked to the ring cavity. However, its dynamical behavior already drastically differs from the behavior of the free-running DFB laser, since the passive optical feedback provided by the robust PM fiber configuration forces the DFB laser to operate preferably in self-injection locking regime. The recorded power fluctuations with typical time scale of a few seconds are caused by environment noise affecting the mutual positions of the optical feedback loop and ring cavity resonances, ν_{LD+FB} and ν_R, respectively. The
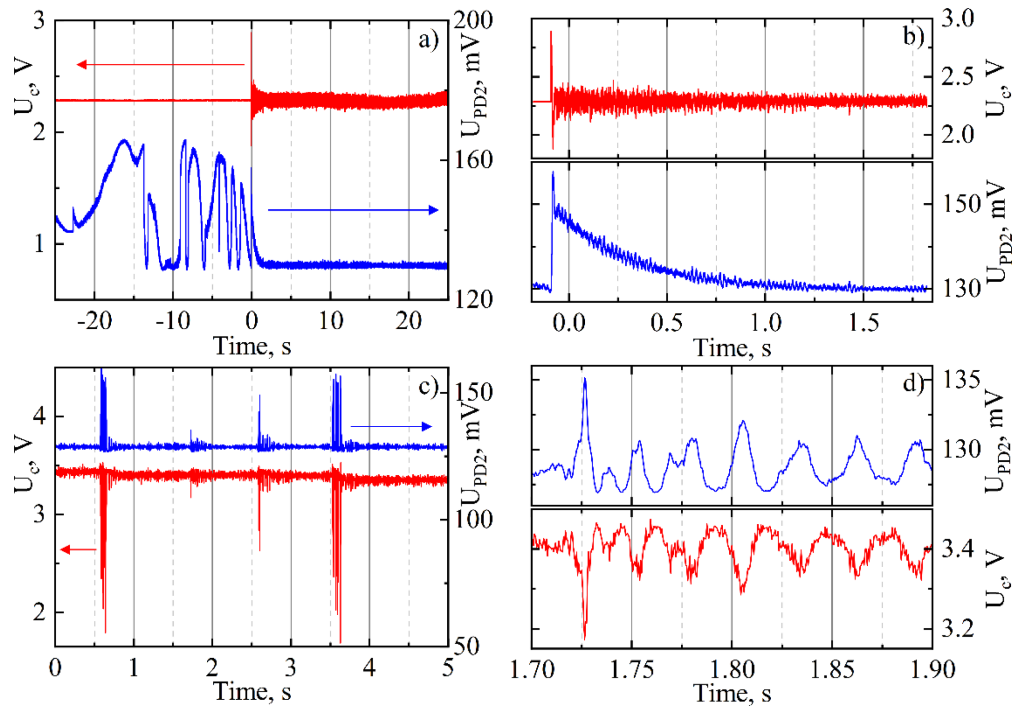
Fig. 4. Oscilloscope traces of the laser output power (the error signal produced by the photodetector) and control voltage applied to the phase shifter before (T<0 s) and after (T>0 s) the optoelectronic feedback activation.

absence of narrow spikes in the oscilloscope trace ensures mode hopping free laser operation in the observed regime.

At $T \approx 0$ s the active feedback is turned on and the voltage applied to the phase-shifter starts to control the laser operation. The challenge addressed to the active optoelectronic feedback circuit is to keep the signal recorded by the photodetector as low as possible applying the suitable driving voltage to the phase shifter. So, the active optoelectronic feedback circuit forces the laser to operate at the laser frequency strongly locked to the high-Q ring cavity resonance thus decreasing the laser output signal. One can see that just after the active circuit is on, the laser power exhibits an exponential decrease down to its new level thus highlighting a transition to the stabilized laser operation. Fig. 3(b) shows the details of the transition process timing a couple of seconds. In the stabilized laser operation regime, the laser power fluctuations are completely suppressed.

The active optoelectronic feedback circuit works against the environmental noise (acoustic and temperature) that is destabilizing the system, affecting the mutual positions of the cavity resonances (ν_R and ν_{LD+FB}). Any deviations of the DFB laser frequency ν_L relative to the ring cavity resonant frequency ν_R increase the laser output power recorded by the photodetector. The electronic feedback circuit controls the voltage applied to the phase shifter maintaining the laser power detected by the photodetector at its minimal value. One can see that at $T > 0$ s the DFB laser frequency is locked to the ring cavity resonance, enabling a stable laser operation.

A particular experiment has been performed to characterize the laser resistance to external perturbations on the laser configuration. Such events may cause mode-hopping in the laser which

in turn destabilizes the laser operation. We have determined time constant characterizing the response of the feedback mechanism to the extensive system disturbances. Fig. 4(c) highlights the effect of four short pencil kicks on the laser board. Its zoom in the interval of 1.7–1.9 s is shown in Fig. 4(d). When the configuration is perturbated, it exhibits a variety of dynamical behaviors that is partially counteracted by the active feedback circuit. Clearly, the system behaves as a high-pass filter, since high frequency acoustic perturbations cannot be compensated by the slow optoelectronic feedback. Following these perturbations, the laser pump power (and so the laser frequency) makes a number of stochastic fluctuations until recoils and returns to the original point in an exponential decay manner. The typical time constant of the feedback mechanism is $\tau_L \sim 0.2$ s.

A specific feature of the laser configuration comprising a ring cavity built from a single coupler is that the optical laser power decreases when the laser gets locked to a ring cavity mode [49]. Fig. 5 compares the laser configuration output power as a function of the laser diode current obtained with an open (green line) and closed (blue line) ring cavity. The red line shows the similar characteristics of the free-running DFB laser. One can see that incorporating the DFB laser into the PM fiber configuration causes 27% losses of laser power due to interconnects between the fiber components. The same happens when the DFB laser is out of resonance with the ring cavity; $\sim$73% of the DFB laser power is emitted through the laser output. Approaching the system to the resonance increases the DFB laser power circulating inside the ring cavity. This increased power is equally shared between light in both polarizations. As a result, the power of the optical feedback signal directed by the polarization beam
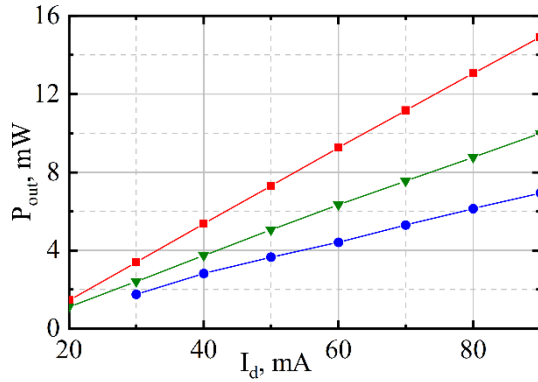
Fig. 5. Power characteristics of the free-running DFB laser (red line), the laser configuration with open ring cavity (green line) and the laser configuration stabilized to operate in the self-injection locking regime (blue line).

splitter to the delay fiber increases, whereas the power redirected to the laser output decreases. In this case, approximately 70% of the residual DFB laser power is emitted by the stabilized laser configuration; ~30% of the residual laser power is spent on the operation of the optical feedback, partially due to its conversion to the orthogonal polarization.

It is worth noting that this laser behavior matches the current understanding of the self-injection locking mechanism in DFB lasers, predicting that the feedback signal is maximized when the laser gets locked to a cavity mode. Specific polarization management used in the PM fiber laser configuration clearly shows that although the laser output power is decreased, the power of the optical feedback signal with orthogonal polarization increases. The same happens in the laser configuration built from non-PM fiber components, where the polarization mapping over the configuration is provided by precise adjustment of two polarization controllers. In those cases, the optical feedback signal is a part of the laser configuration output possessing the polarization state orthogonal to that of the DFB laser. Whether the polarization distribution is not taken into account, it looks like the injection locking is accompanied by a decrease in the optical feedback signal, provoking a misunderstanding [49].

B. Self-Heterodyne Optical Spectra

A delayed self-heterodyne technique [53], [54], [55] has been employed to measure the linewidth of radiation emitted by the laser at different stabilization regimes. An all-fiber disbalanced Mach–Zehnder interferometer with a 50.5 km delay fiber and 80 MHz acousto-optic phase modulator supplied by polarization controller is used for this purpose. The beat signal from the interferometer is detected by a ~ 5 GHz photodiode and RF spectrum analyzer (FSH8, Rohde & Schwarz).

Fig. 6 compares the experimental self-heterodyne optical spectra recorded with the free-running DFB laser (a) and with the DFB laser stabilized to operate in self-injection regime by active optoelectronic feedback (b). The shown spectra are centered around ~ 80 MHz and averaged over 10 realizations each. One can see that self-injection locking causes more than 1000-fold narrowing of the laser spectrum. To proceed the

measured data, we use the method based on the decomposition of the self-heterodyne spectra into Gaussian and Lorentzian contributions. In this approach, the laser's line is thought to be Gaussian in the range near the top, and Lorentzian in the wings [54]. Long delay fiber results in considerable broadening of the self-heterodyne spectrum due to the 1/f frequency noise. The convolution with the acquired 1/f noise causes overestimation of the natural laser linewidth, if it is estimated from the 3-dB width of self-heterodyne spectrum as commonly used. Since, the 1/f noise contributes Gaussian broadening mostly pronounced near the top of the laser spectrum, the estimation by the -20 dB width of self-heterodyne spectrum is closer to the natural laser linewidth, however, the result is still overestimating. The measured self-heterodyne spectrum is actually the Voigt function, i.e., the convolution of the Lorentzian and Gaussian spectra. The Lorentzian and Gaussian contributions are evaluated by fitting the measured self-heterodyne spectrum by the Voigt profile. Fig. 6 shows the fitting Voigt profiles obtained using the algorithm described in Ref. [55]. One can see that the fitting is applied just to the highest points in the wings ensuring upper values of the Lorentzian laser linewidths estimated for two laser outputs. The Lorentzian laser linewidth Δw_L is a half of the Lorentzian width (FWHM) w_L of self-heterodyne spectrum and the Gaussian component Δw_G is $\sqrt{2}/2$ times the Gaussian linewidth (FWHM) w_G of self-heterodyne spectrum [54]. Therefore, the Gaussian laser linewidths are found to be ~ 1.4 MHz for the free laser and narrower than ~ 2.5 kHz for the stabilized laser. The natural Lorentzian laser linewidths are ~ 430 kHz for the free laser and narrower than ~ 75 Hz for the stabilized laser.

C. Noise Performance

Fig. 7 compares the noise performance of the free-running and actively stabilized self-injection locked DFB-lasers. Fig. 7(a) shows the relative intensity noise (RIN) of the lasers measured in 10 Hz $-$ 1 MHz frequency range. In fact, the RIN is the power spectrum density (PSD) of the intensity fluctuation expressed as the Fourier transform of the autocorrelation function of power fluctuations normalized to the mean power signal:

$$S_I(f) = \frac{2}{\overline{P}^2} \int_{-\infty}^{+\infty} \langle \delta P(t)\, \delta P(t+\tau) \rangle \, \exp\left(i2\pi f\tau\right)\, \mathrm{d}\tau \quad (1)$$

Here $S_I(f)$ is the one-sided PSD, $\overline{P}$ is the mean value of the laser power, $\delta P(t)$ is the power deviation from the mean value, f is the noise frequency, τ is the delay time.

To evaluate the RIN, laser power traces of 100 milliseconds, containing 10 million points, are recorded using a digital oscilloscope (Agilent MSO9404A) and subsequently processed using (1). The running averages of these distributions for both the free-running and actively stabilized self-injection locked DFB laser are represented by the red and blue lines, respectively. One can see that incorporating the DFB laser into the fiber configuration impairs the RIN value of the free-running DFB laser by only $1 - 2$ dBc/Hz. We believe that this is attributable to the relatively slow response time (on the order of milliseconds) of the active feedback circuit which counters the laser power
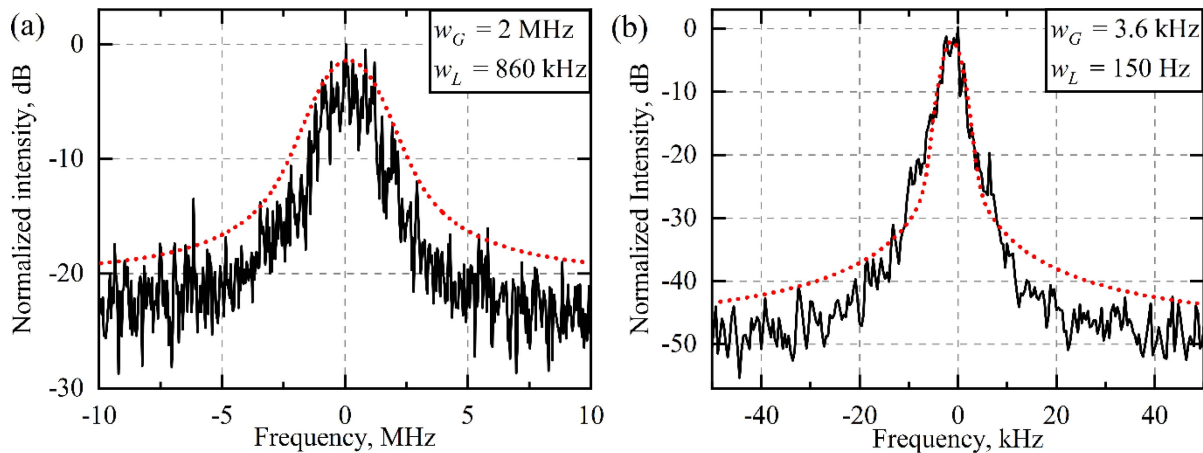
Fig. 6.   Delayed self-heterodyne spectra of the free-running DFB laser (a) and the DFB laser stabilized to operate in the self-injection locking regime (b). The measured spectra (black) and their fitting Voigt profiles (red dotted line) with the Gaussian (w_G) and Lorentzian (w_L) linewidths (FWHM) used as the fitting parameters.
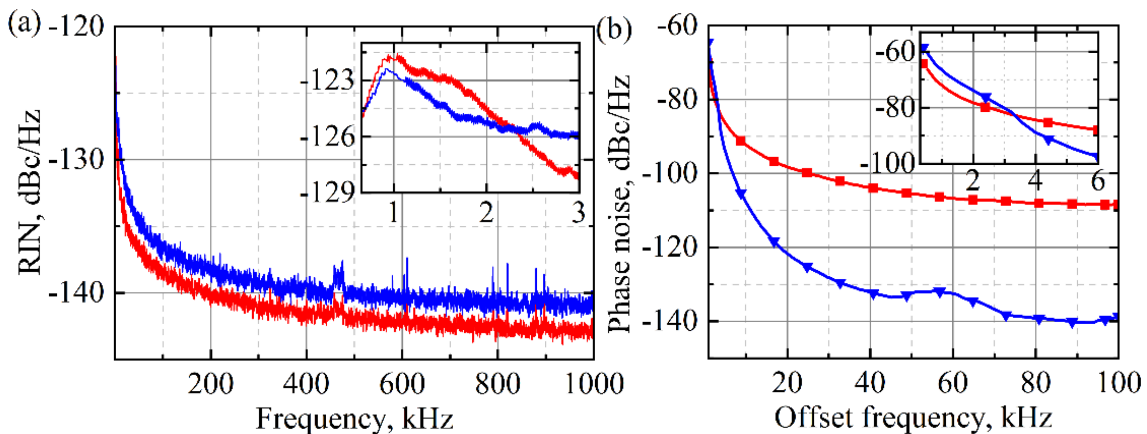

Fig. 7.   Phase (a) and relative intensity (b) noise of the free-running DFB laser (red lines) and the DFB laser stabilized to operate in the self-injection locking regime (blue lines).

fluctuations. This impairment has only a minor effect on the laser output RIN that is mainly determined by the noise performance of the laser power supply. Beyond 10 kHz, the active stabilization circuit maintains the RIN of the laser below − 130 dBc/Hz. At low-frequencies (less than 2.5 kHz, i.e., in time scales longer than the response time of the phase shifter), a reduction in relative intensity noise is observed compared to the free-run DFB laser.

Fig. 7(b) shows the one-sided power spectral density (PSD) of phase noise, recorded with an RF spectrum analyzer (R&S FSP40) in the range of 1 – 100 kHz. These PSDs have been measured using the self-heterodyne method [56], [57], [58], relying on the interferometer described in the previous section but with 1-km delayed fiber. Beyond 30 kHz, one can see that the active stabilization circuit maintains the phase noise of the pump radiation below − 130 dBc/Hz. Across this range, the phase noise from the actively stabilized laser is substantially (by up to ∼ 35dBc/Hz) lower than that of the free-running DFB-laser. Within the utilized RF spectrum range, the noise

generated by the feedback loop has a negligible impact on laser performance. However, it becomes noticeable at extremely low frequencies (less than 1 kHz, as seen in the inset). The marked enhancement in laser performance, when compared to previous works [37], [38], [49], can be attributed to the filtering effect in the high-Q-factor ring cavity, as well as the increased stability of the laser configuration due to its PM fiber design, thermal control and vibro-isolation.

D. Frequency Drift

Subsequent experiments explore the impact of thermal stabilization of the laser configuration as a whole. Environmental temperature fluctuations are the primary source of laser instabilities in the self-injection locking regime. When the temperature noise forces the resonant frequency of the high-Q fiber ring cavity to drift, the DFB laser frequency drifts in tandem. To counter the laser frequency drift, the insulated box containing the laser configuration is supplied with a thermal stabilization circuit,
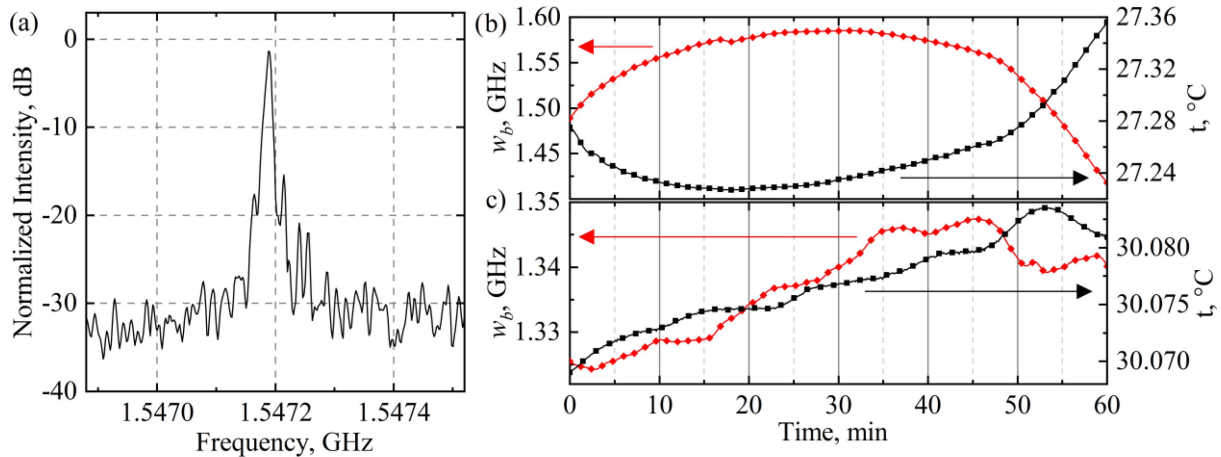
Fig. 8. Measurements of the laser frequency drift. (a) RF beat spectrum acquired for ~20ms; (b, c) evolution of the RF beat spectrum peak frequency measured without (b) and with (c) active stabilization for 60 minutes (black curves) shown in a comparison with the instantaneous temperature (red curves).

maintaining the temperature of the laser box at a predetermined value $\sim 30 \pm 0.01$ ^{0}C.

To evaluate the frequency drift in the stabilized self-injection locked laser, we used a beat signal combining the laser output with an etalon narrow-band sub-kilohertz source (TeraXion Inc.). The etalon laser is specified to operate at close frequency with a laser linewidth of 6 kHz and frequency drift better than $\sim$ 1 MHz/min. The RF signal analyzer (R&S FSP40, 40 GHz) permanently monitors the radiofrequency (RF) beat spectrum. Fig. 8(a) presents a typical RF spectrum recorded with an acquisition time of 20 ms. The spectrum exhibits a pronounced peak at $\sim$ 1.5472 GHz with a width of 6 kHz, primarily determined by the TeraXion laser linewidth. Fig. 8(b) and (c) depict the time evolution of the beat spectrum peak frequency for approximately 1 hour, recorded for thermally non-stabilized (c) and stabilized (d) laser boxes. These data are compared to the absolute temperature permanently monitored in the laser box. One can see that, without thermal stabilization, the laser operation frequency closely reproduces the temperature variations. The laser frequency and temperature change in an anti-phase manner, ensuring the proportionality between the changes with the factor of ~ -1.33 GHz/$^{\circ}$C. So, the beat signal frequency drift is entirely determined by the drift of the environmental temperature in the laser box. It is estimated to be $\sim$ 4–5 MHz/min and comparable to the frequency drifts reported with the self-injection locked lasers earlier.

The temperature control reduces the beat frequency drift as shown in Fig. 8(b) by an order of magnitude, down to $\sim$ 0.5 MHz/min. It is lower than the frequency drift specified by the used commercial laser. One can check that, in this case, the change in beat frequency with temperature superposes two qualitatively behaviors - a slow positive monotonic increase and a faster anti-phase response to temperature fluctuations (as ~ -1.33 GHz/$^{\circ}$C) that are contributed by two different laser sources — the commercial and experimental lasers, respectively. This analysis reveals that the absolute self-injection-locked laser frequency deviation range is better than 8 MHz. We believe this range can be further reduced, at least by an order of magnitude,

by supplying the laser configuration with more precise thermal control.

V. DISCUSSION

We have introduced a simple narrow-band laser configuration based on a DFB laser coupled to an all-fiber ring cavity that operates in the self-injection-locking regime. A low-cost USB-DAQ is used to stabilize the laser system preventing mode-hopping. Importantly, the self-injection locking mechanism ensures continuous coupling between the DFB laser and the external fiber ring cavity, enabling exceptional low-noise narrow-band lasing. Unlike previous laser designs, the new laser configuration is entirely spliced from PM fiber components. Furthermore, similar to [49], we employed a fiber ring cavity constructed (and subsequently integrated into the configuration) using just one fiber coupler, instead of the two couplers utilized in many earlier configurations. Such a cavity design potentially reduces optical losses in the ring cavity (by a factor of two compared to [38], offering an enhanced Q-factor.

Thanks to the new laser design, the performance characteristics of the laser have been significantly improved. The laser's Lorentzian linewidth has been reduced to approximately 75 Hz from the 400 Hz measured earlier in the same manner. To the best of our knowledge, this is the narrowest laser linewidth reported for DFB lasers that are self-injection locked to an external fiber cavity [33]. The PM laser's performance is impressive, especially considering that no expensive components were used for stabilization. The laser output power of approximately 8 mW allows for potential scaling with external amplifiers. The laser's operational frequencies are firmly locked to the ring cavity resonances, and the drift observed in our experiments is primarily influenced by environmental temperature variations. By applying thermal control to the entire laser configuration, we've reduced the laser frequency drift to roughly 0.5 MHz/min, ensuring absolute fluctuations of the laser frequency are less than 8 MHz. Earlier, the limiting factor was the mechanical piezo-actuator, which produced acoustic noise in the feedback

fiber loop. Replacing the piezo-actuator with a thermo-optical phase shifter eliminated this acoustic noise, further minimizing the laser noise and frequency drift. Utilizing the PM fiber configuration negates the need for polarization controllers, making the laser setup more robust and adjustment-free. Compared to a non-PM configuration, the laser's noise performance improved by ~ 10 dBc/Hz and ~ 50 dBc/Hz for the measured RIN and phase noise PSD, respectively.

In general, our results enhance the understanding of the self-injection-locking mechanism in semiconductor lasers, offering novel avenues for manipulating and controlling their properties. In particular, we have explained the specific operations of the feedback mechanism in laser configurations comprising a ring cavity built from a single coupler. Prior examinations of the non-PM laser setup [49] have emphasized its distinct differences from other configurations. In most laser configurations, the feedback signal is maximized when the laser is synchronized with a cavity mode. However, in setups with a single coupler cavity, the laser output used for feedback takes its minimum value. This has led to questions about whether the same mechanism governs the laser's self-injection locking. We have analyzed this mechanism in the PM fiber configuration, finding no contradictions between the observed feature and our current understanding. In the PM fiber configuration, the laser output power is divided by polarization between two channels, and only one is used for optical feedback, enabling the DFB laser's self-injection locking. Thus, when the laser locks to the ring cavity mode, the optical feedback signal maximizes like other laser configurations, even though the total laser output power (in both polarizations) could reach its minimum. The same takes place in the setup built from non-PM fiber components, where the consistent polarization mapping across the configuration is provided by the precise adjustment of two polarization controllers. The optical feedback signal is the component with a polarization state orthogonal to the DFB laser's polarization state. Its power increases when the laser is locked to the ring cavity. However, the total laser power recorded by the photodetector at the laser output decreases, leading to some confusion. It may seem as though the injection locking results in a reduction in the optical feedback signal. However, our new experiments with the PM laser configuration have explained that this is not the case.

VI. Conclusion

In conclusion, we have implemented an active feedback loop utilizing a low-cost USB-DAQ in a configuration where a DFB laser is self-injection-locked to an external all-fiber ring resonator. Notably, the laser configuration is entirely spliced from polarization maintaining (PM) single-mode optical fiber, which offers significantly improved stability against environmental noise. Our findings enhance the understanding of the self-injection-locking mechanism in semiconductor lasers, paving the way for new possibilities in manipulating and controlling their properties. The newfound capability to generate a sub-100 Hz laser linewidth is particularly appealing for a myriad of laser applications, including high-resolution spectroscopy, phase coherent optical communications, microwave photonics,

coherent optical spectrum analyzers, and distributed fiber optics sensing — especially in phase-OTDR acoustic sensing. We believe our findings will stimulate design of PM fiber-based Brillouin laser configurations enabling further progress in laser linewidth narrowing. Looking ahead, adapting the proposed laser design to integrated photonics [22], [59], [60], [61], [62], [63], [64], [65] promises to dramatically reduce both costs and footprints across various applications, from ultra-high-capacity fiber and data center networks to atomic clocks and microwave photonics.

References

[1] Y. H. Lai et al., "Ultra-narrow-linewidth lasers for quantum applications," in *Proc. IEEE Conf. Lasers Electro-Opt.*, 2022, pp. 1–2.

[2] A. Zhang, X. Feng, M. Wan, Z. Li, and B.-O. Guan, "Tunable single frequency fiber laser based on FP-LD injection locking," *Opt. Exp.*, vol. 21, pp. 12874–12880, 2013.

[3] C. Wang et al., "Boron quantum dots all-optical modulator based on efficient photothermal effect," *Opto-Electron. Adv.*, vol. 4, 2021, Art. no. 200032.

[4] J. Geng, L. Yang, S. Zhao, and Y. Zhang, "Resonant micro-optical gyro based on self-injection locking," *Opt. Exp.*, vol. 28, pp. 32907–32915, 2020.

[5] Y. Zhang, J. Geng, L. Li, Y. Wang, and L. Yang, "Exceptional-point-enhanced Brillouin micro-optical gyroscope based on self-injection locking," *Opt. Commun.*, vol. 528, 2023, Art. no. 129008.

[6] F. Karim, A. F. Mitul, B. Zhou, and M. Han, "High-Sensitivity demodulation of fiber-optic acoustic emission sensor using self-injection locked diode laser," *IEEE Photon. J.*, vol. 14, no. 4, Aug. 2022, Art. no. 7142610.

[7] D. Claus, I. Alekseenko, M. Grabherr, G. Pedrini, and R. Hibst, "Snap-shot topography measurement via dual-VCSEL and dual wavelength digital holographic interferometry," *Light: Adv. Manuf.*, vol. 2, 2021, Art. no. 29.

[8] J. L. Bueno Escobedo et al., "Self-injection locking of the DFB laser through an external ring fiber cavity: Application for phase sensitive OTDR acoustic sensor," *Results Phys.*, vol. 7, pp. 641–643, 2017.

[9] R. Amin, J. Greenberg, B. Heffernan, T. Nagatsuma, and A. Rolland, "Exceeding octave tunable terahertz waves with zepto-second level timing noise," 2022, *arXiv:2207.07750v1*.

[10] Z. Bai et al., "Narrow-linewidth laser linewidth measurement technology," *Front. Phys.*, vol. 9, 2021, Art. no. 25461.

[11] E. Fomiryakov, D. Kharasov, S. Nikitin, O. Nanii, and V. Treshchikov, "New approach to laser characterization using delayed self-heterodyne interferometry," *J. Lightw. Technol.*, vol. 39, no. 15, pp. 5191–5196, Aug. 2021.

[12] T. Hansch and B. Couillaud, "Laser frequency stabilization by polarization spectroscopy of a reflecting reference cavity," *Opt. Commun.*, vol. 35, pp. 441–444, 1980.

[13] J. Alnis, A. Matveev, N. Kolachevsky, T. Udem, and T. Hänsch, "Subhertz linewidth diode lasers by stabilization to vibrationally and thermally compensated ultralow-expansion glass Fabry-Pérot cavities," *Phys. Rev. A*, vol. 77, 2008, Art. no. 053809.

[14] D. Brunner, R. Luna, A. Delhom i Latorre, X. Porte, and I. Fischer, "Semiconductor laser linewidth reduction by six orders of magnitude via delayed optical feedback," *Opt. Lett.*, vol. 42, pp. 163–166, 2017.

[15] K. Petermann, *Laser Diode Modulation and Noise*, vol. 3. New York, NY, USA: Springer Science & Business Media, 2012.

[16] K. Petermann, "External optical feedback phenomena in semiconductor lasers," *IEEE J. Sel. Topics Quantum Electron.*, vol. 1, no. 2, pp. 480–489, Jun. 1995.

[17] J. Ohtsubo, *Semiconductor Lasers: Stability, Instability and Chaos*, vol. 111. New York, NY, USA: Springer, 2012.

[18] R. Galiev et al., "Spectrum collapse, narrow linewidth, and bogatov effect in diode lasers locked to high-Q optical microresonators," *Opt. Exp.*, vol. 26, pp. 30509–30522, 2018.

[19] W. Liang et al., "Ultralow noise miniature external cavity semiconductor laser," *Nature Commun.*, vol. 6, pp. 1–6, 2015.

[20] D. Huang et al., "High-power sub-kHz linewidth lasers fully integrated on silicon," *Optica*, vol. 6, pp. 745–752, 2019.

[21] S. Shao, J. Li, Y. Wu, S. Yang, H. Chen, and M. Chen, "Modulation bandwidth enhanced self-injection locking laser with an external high-Q microring reflector," *Opt. Lett.*, vol. 46, pp. 3251–3254, 2021.

[22] N. M. Kondratiev et al., "Recent advances in laser self-injection locking to high-Q microresonators," *Front. Phys.*, vol. 18, 2023, Art. no. 21305.

[23] D. A. Korobko, I. O. Zolotovskii, K. Panajotov, V. V. Spirin, and A. A. Fotiadi, "Self-injection-locking linewidth narrowing in a semiconductor laser coupled to an external fiber-optic ring resonator," *Opt. Commun.*, vol. 405, pp. 253–258, 2017.

[24] V. Spirin, C. López-Mercado, P. Mégret, and A. Fotiadi, "Single-mode brillouin fiber laser passively stabilized at resonance frequency with self-injection locked pump laser," *Laser Phys. Lett.*, vol. 9, 2012, Art. no. 377.

[25] V. V. Spirin, C. A. López-Mercado, D. Kinet, P. Mégret, I. O. Zolotovskiy, and A. A. Fotiadi, "A single-longitudinal-mode Brillouin fiber laser passively stabilized at the pump resonance frequency with a dynamic population inversion grating," *Laser Phys. Lett.*, vol. 10, 2013, Art. no. 015102.

[26] C. A. López-Mercado et al., "Locking of the DFB laser through fiber optic resonator on different coupling regimes," *Opt. Commun.*, vol. 359, pp. 195–199, 2016.

[27] Z. Fang, H. Cai, G. Chen, and R. Qu, *Single Frequency Semiconductor Lasers*. New York, NY, USA: Springer, 2017.

[28] F. Wei et al., "Subkilohertz linewidth reduction of a DFB diode laser using self-injection locking with a fiber Bragg grating Fabry-Perot cavity," *Opt. Exp.*, vol. 24, pp. 17406–17415, 2016.

[29] S. Huang et al., "Dual-cavity feedback assisted DFB narrow linewidth laser," *Sci. Rep.*, vol. 7, 2017, Art. no. 1185.

[30] J. - J. Chen et al., "Multi-wavelength injection locked semiconductor comb laser," *Photon. Res.*, vol. 10, pp. 1840–1847, 2022.

[31] K. Kasai, M. Nakazawa, M. Ishikawa, and H. Ishii, "8 kHz linewidth, 50 mW output, full C-band wavelength tunable DFB LD array with self-optical feedback," *Opt. Exp.*, vol. 26, pp. 5675–5685, 2018.

[32] A. F. Mitul and M. Han, "Wavelength drift suppression of a semiconductor laser with filtered optical feedback from a fiber-optic loop using active phase-delay control," *Opt. Lett.*, vol. 47, pp. 5457–5460, 2022.

[33] M. Zou et al., "Sub-kHz-linewidth laser generation by self-injection locked distributed feedback fiber laser," *Opt. Laser Technol.*, vol. 169, 2024, Art. no. 110022.

[34] J. Geng, L. Yang, J. Liang, S. Liu, and Y. Zhang, "Stability in self-injection locking of the DFB laser through a fiber optic resonator," *Opt. Commun.*, vol. 505, 2022, Art. no. 127531.

[35] J. L. Bueno Escobedo, V. V. Spirin, C. A. López-Mercado, P. Mégret, I. O. Zolotovskii, and A. A. Fotiadi, "Self-injection locking of the DFB laser through an external ring fiber cavity: Polarization behavior," *Results Phys.*, vol. 6, pp. 59–60, 2016.

[36] J. L. Bueno Escobedo et al., "Distributed measurements of vibration frequency using phase-OTDR with a DFB laser self-stabilized through PM fiber ring cavity," *Results Phys.*, vol. 12, pp. 1840–1842, 2019.

[37] V. V. Spirin, J. L. B. Escobedo, D. A. Korobko, P. Mégret, and A. A. Fotiadi, "Stabilizing DFB laser injection-locked to an external fiber-optic ring resonator," *Opt. Exp.*, vol. 28, pp. 478–484, 2020.

[38] V. V. Spirin, J. L. Bueno Escobedo, D. A. Korobko, P. Mégret, and A. A. Fotiadi, "Dual-frequency laser comprising a single fiber ring cavity for self-injection locking of DFB laser diode and Brillouin lasing," *Opt. Exp.*, vol. 28, pp. 37322–37333, 2020.

[39] M. H. Idjadi and F. Aflatouni, "Integrated Pound-Drever-Hall laser stabilization system in silicon," *Nature Commun.*, vol. 8, 2017, Art. no. 1209.

[40] X. - L. Zhou et al., "Active stabilization of multi-parameter in AMO experiments with a single digital servo," *Opt. Laser Technol.*, vol. 167, 2023, Art. no. 109791.

[41] C. A. Lopez-Mercado, D. A. Korobko, I. O. Zolotovskii, and A. A. Fotiadi, "Application of dual-frequency self-injection locked dfb laser for brillouin optical time domain analysis," *Sensors*, vol. 21, 2021, Art. no. 6859.

[42] V. V. Spirin, M. Castro, C. A. López-Mercado, P. Mégret, and A. A. Fotiadi, "Optical locking of two semiconductor lasers through high-order Brillouin Stokes components in optical fiber," *Laser Phys.*, vol. 22, pp. 760–764, 2012.

[43] C. E. Preda, A. A. Fotiadi, and P. Megret, "Numerical approximation for Brillouin fiber ring resonator," *Opt Exp.*, vol. 20, pp. 5783–5788, 2012.

[44] D. Korobko et al., "Detuning effects in Brillouin ring microresonator laser," *Opt. Exp.*, vol. 28, pp. 4962–4972, 2020.

[45] V. V. Spirin, J. Kellerman, P. L. Swart, and A. A. Fotiadi, "Intensity noise in SBS with injection locking generation of stokes seed signal," *Opt. Exp.*, vol. 14, pp. 8328–8335, 2006.

[46] N. T. Otterstrom, R. O. Behunin, E. A. Kittlaus, Z. Wang, and P. T. Rakich, "A silicon Brillouin laser," *Science*, vol. 360, pp. 1113–1116, 2018.

[47] C. A. López-Mercado et al., "Accuracy of single-cut adjustment technique for double resonant Brillouin fiber lasers," *Opt. Fiber Technol.*, vol. 20, pp. 194–198, 2014.

[48] Z. Zhong et al., "Photonic millimeter wave generation and stabilization in optically injected discrete-mode semiconductor lasers subject to photonic filter feedback," *J. Lightw. Technol.*, vol. 41, no. 17, pp. 5632–5640, Sep. 2023.

[49] V. V. Spirin et al., "Sub-kilohertz Brillouin fiber laser with stabilized self-injection locked DFB pump laser," *Opt. Laser Technol.*, vol. 141, 2021, Art. no. 107156.

[50] M. A. Soto, *Distributed Brillouin Sensing: Time-Domain Techniques*. Singapore: Springer, 2018.

[51] L. Rossi, F. Bastianini, and G. Bolognini, "Study of injection-locked stabilized, short cavity Brillouin ring laser source design for fiber sensing applications," *J. Rapid Pub. - J. Eur. Opt. Soc.*, vol. 18, 2022, Art. no. 5.

[52] L. Rossi, D. Marini, F. Bastianini, and G. Bolognini, "Analysis of enhanced-performance fibre Brillouin ring laser for Brillouin sensing applications," *Opt. Exp.*, vol. 27, pp. 29448–29459, 2019.

[53] D. Derickson, C. Hentschel, and J. Vobis, *Fiber Optic Test and Measurement*, vol. 8. Hoboken, NJ, USA: Prentice Hall PTR, 1998.

[54] L. B. Mercer, "1/f frequency noise effects on self-heterodyne linewidth measurements," *IEEE Lightw. Technol.*, vol. 9, no. 4, pp. 485–493, Apr. 1991.

[55] M. Chen, Z. Meng, J. Wang, and W. Chen, "Ultra-narrow linewidth measurement based on Voigt profile fitting," *Opt. Exp.*, vol. 23, pp. 6803–6808, 2015.

[56] S. Camatel and V. Ferrero, "Narrow linewidth CW laser phase noise characterization methods for coherent transmission system applications," *J. Lightw. Technol.*, vol. 26, no. 17, pp. 3048–3055, Sep. 2008.

[57] O. Llopis, P. H. Merrer, H. Brahimi, K. Saleh, and P. Lacroix, "Phase noise measurement of a narrow linewidth CW laser using delay line approaches," *Opt. Lett.*, vol. 36, pp. 2713–2715, 2011.

[58] Y. Li et al., "Laser frequency noise measurement using an envelope-ratio method based on a delayed self-heterodyne interferometer," *Opt. Commun.*, vol. 435, pp. 244–250, 2019.

[59] J. Ling et al., "Self-injection locked frequency conversion laser," *Laser Photon. Rev.*, vol. 9, 2023, Art. no. 2200663.

[60] L. Dang et al., "Ultra-high spectral purity laser derived from weak external distributed perturbation," *Opto-Electron. Adv.*, vol. 6, 2023, Art. no. 210149.

[61] D. Marpaung, J. Yao, and J. Capmany, "Integrated microwave photonics," *Nature Photon.*, vol. 13, pp. 80–90, 2019.

[62] W. Jin et al., "Hertz-linewidth semiconductor lasers using CMOS-ready ultra-high-Q microresonators," *Nature Photon.*, vol. 15, pp. 346–353, 2021.

[63] C. Xiang, W. Jin, and J. E. Bowers, "Silicon nitride passive and active photonic integrated circuits: Trends and prospects," *Photon. Res.*, vol. 10, pp. A82–A96, 2022.

[64] S. Gundavarapu et al., "Sub-hertz fundamental linewidth photonic integrated Brillouin laser," *Nature Photon.*, vol. 13, pp. 60–67, 2019.

[65] Z. Zhou et al., "Prospects and applications of on-chip lasers," *eLight*, vol. 3, pp. 1–25, 2023.